ELSEVIER

Contents lists available at ScienceDirect

Materials Science & Engineering B

journal homepage: www.elsevier.com/locate/mseb



Influence of nanoparticle size on ethanol gas sensing performance of mesoporous α -Fe₂O₃ hollow spheres



Changqing Jin^{a,*}, Chenghai Ge^a, Gang Xu^a, George Peterson^b, Zengyun Jian^a, Yongxing Wei^a, Kexin Zhu^a

- ^a School of Materials and Chemical Engineering, Xi'an Technological University, Xi'an 710021, People's Republic of China
- b University of Nebraska Lincoln, Department of Mechanical and Materials Engineering, W342NH, Lincoln, NE 68588-0526, USA

ARTICLE INFO

Keywords: Fe_2O_3 Hollow spheres Template Sensors Mesoporous Crystal growth

ABSTRACT

Mesoporous $\alpha\text{-Fe}_2O_3$ hollow spheres were synthesized through a heterogeneous nucleation method which incorporates a template for carbon-sphere nucleation. The grain size and grain size distribution of nanoparticles that assemble in hollow spheres could be controlled by the precursor solution concentration of Fe³⁺. The sensitivity of the samples to ethanol gas was investigated. The results indicated that the gas sensing performance is a function of grain size and grain size distribution, which is related to the concentration of Fe³⁺. The device sensitivity first increases, then decreases according to grain size. It was found that an average grain size of 15.9 \pm 1.4 nm has the highest sensitivity to ethanol gas.

1. Introduction

Metal oxide gas sensors have been developed over the last decade [1-6]. Ferric oxide (Fe_2O_3) is a popular n-type semiconductor within this field because it has promising physical and chemical properties. Ferric oxide is abundant, widely available, non-toxic in nature, and has a low production cost; all properties which make it popular for use in photo-electrodes [7,8], photocatalytic water splitting [9], super capacitors [10], gas sensors [11], and adsorbent materials of heavy metal ions [12], to name a few.

In the field of gas sensors, improved performance is generally attributed to improved crystallinity, an exposed crystal plane with high energy, increased surface defects and/or increased specific surface area. With those attributes in mind, several kinds of alpha-Fe₂O₃ (α-Fe₂O₃) nanostructures have been examined to look for enhancements in gas sensing performance. Such structures have included hierarchical flowers [13], porous nanoplates [14], nano-urchins [15], nano-heterostructures [2,16] and hollow spheres [6,17]. We now seek to design a material, building upon the previous research, which has advantageous chemical and physical properties. One of the more obvious ways to accomplish increased sensor performance is by increasing the specific surface area utilizing a hollow morphology and structure. It is believed that a hollow nanostructure belonging to the mesoporous category – a structure with pores in the size range of 2–50 nm – will result in a larger specific surface area than other nanostructures. Moreover, the unique nanostructure provides efficient molecular transport

In this paper, we show that mesoporous $\alpha\text{-Fe}_2O_3$ hollow spheres of varying GS are prepared by a carbon sphere template method, and that GS distribution may be controlled by the concentration of ferric nitrate (Fe(NO_3)_3) in an alcohol solution. Furthermore, the relationship between GS, GS distribution and SR were investigated. This study seeks to provide new insight into the influence of GS on gas sensing performance.

2. Experimental

Mesoporous α-Fe2O3 hollow spheres were synthesized by a

E-mail address: eaglejin@xatu.edu.cn (C. Jin).

pathways to the interior surface. To date, little effort has been made to identify the relationship between the sensor response (SR) and grain size (GS) and GS distribution. This is understandable as controlling the GS (< 20 nm) and GS distribution requires controlling a complex nucleation and growth process in a precise manor. Hollow nanosphere synthesis may be accomplished either heterogeneously or homogeneously, i.e. with or without a nucleation template. Liu et al. synthesized hollow nanostructures with different morphologies by a template-free hydrothermal method (homogeneous nucleation) [18]. While, a template method allows heterogeneous nucleation on the template to be the preferential source of nucleation, spontaneous nucleation within the solution (homogeneous nucleation) is possible. With two mechanisms for nucleation and growth, quantification of GS distribution must include the identification and distinction between heterogeneous and homogeneous nucleation and growth.

^{*} Corresponding author.

template technique that was reported in our previous work [19]. Carbon spheres were prepared utilizing a hydrothermal method. First, 6.44 g glucose (China National Medicines Corporation Ltd) was dissolved in 65 ml deionized water and magnetically stirred for 30 min. Then, the solution was transferred to a 100 ml Teflon-lined stainless steel autoclave. With the dissolved glucose providing the carbon constituent and the Teflon being permeable to oxygen, the hydrothermal reaction was completed by maintaining the autoclave at 180 °C for 9 h. The resulting precipitate of carbon spheres was then collected and washed using a centrifuge with ethyl alcohol (China National Medicines Corporation Ltd) and deionized water, followed by desiccation at 80 °C for 6 h.

The mesoporous α -Fe₂O₃ hollow spheres synthesis begins with 0.20 g carbon spheres (collected above) dispersed (by sonication for 30 min) into a 40 ml ethanol solution containing Fe(NO₃)₃ (China National Medicines Corporation Ltd) of varying molar concentration. The suspension was magnetically stirred for 12 h at room temperature, followed by centrifuging repeatedly with ethanol. Finally, the obtained products were desiccated at 80 °C for 5 h, and calcined in air at 550 °C for 4 h with a heating rate of 4 °C/min. 0.0375, 0.0750, 0.1125, 0.1500 and 0.1875 mol/L Fe(NO₃)₃ ethanol solutions were used to prepare hollow spheres. The samples were named S1, S2, S3, S4 and S5, respectively.

The crystal structures of the samples were determined by X-ray diffraction (XRD, XRD-6000, with high-intensity Cu Ka radiation with a wavelength of 0.15406 nm). The morphologies and GS were analyzed by scanning electron microscopy (SEM, Quanta 400F) and transmission electron microscopy (TEM, JEM-2010). The inner architectures and specific area of the mesoporous α-Fe2O3 hollow spheres were ex-Brunauer-Emmett-Teller amined by (BET) nitrogen adsorption-desorption (Nova 2000E). Pore-size distribution was determined from the adsorption branch of the isotherms using the Barett-Joyner-Halenda (BJH) method. Gas sensing property measurements were performed utilizing a static test system (WS-30A, Winsen Electronics Co. Ltd., Zheng Zhou, China). The SR was defined as Ra/Rg, where Ra is the resistance of the sensor in air and Rg is the resistance of the sensor in a test gas. The response and recovery time is defined as the time for the sensor to reach 90% of its maximum response and fall to 10% of its maximum response, respectively [3]. The relative humidity at the time of measurement was 25%.

3. Results and discussion

XRD patterns of the products are shown in Fig. 1. All diffraction

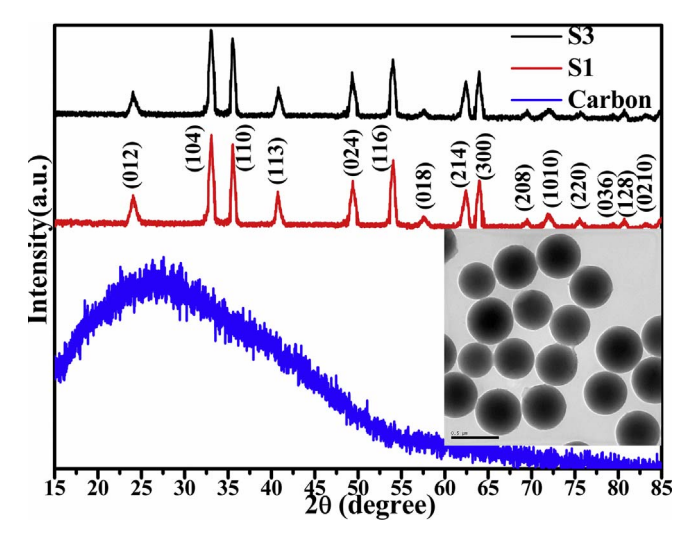


Fig. 1. XRD patterns of samples. Indexing matches that of $\alpha\text{-Fe}_2O_3$. Inset shows TEM image of carbon sphere templates.

peaks are easily indexed to pure $\alpha\text{-Fe}_2O_3$ with the lattice parameters of $a=b=5.034\,\text{Å},\ c=13.746\,\text{Å}$ and a space group of R-3c (1 6 7) (JCPDS NO. 79–1741). The XRD pattern of the carbon spheres has a broad asymmetrical peak centered between 20 and 45°. This corresponds to carbon with a combination of sp^2 (26.6° corresponding to 0.335 nm between planes) [20] and sp^3 (43.9° corresponding to the (1 1 1) plane spacing of 0.206 nm) lattice structures in the grains that combine to form the hollow spheres which have no long range order [21]. TEM, inset of Fig. 1, show that the average diameter for a carbon sphere template is about 450 nm and that the carbon sphere template size distribution is uniform.

TEM and SEM were utilized to characterize the morphology of the mesoporous α-Fe₂O₃ hollow spheres, which are shown in Fig. 2. The diameter of the mesoporous α-Fe₂O₃ hollow spheres is about 300 nm, which is smaller than the diameter of the carbon spheres. The shrinkage could be attributed to dehydration and oxidation of the carbon spheres. Fig. 2a and b show a typical branching structure (arrows a and b) along with images of damaged spheres (arrows c and d), which are not found in Fig. 2d-e. Fig. 2a-d indicate that the density of porosity is gradually increasing, and the scale of porosity and GS is gradually decreasing. Agglomerating nanoparticles (arrow e, f and g) are shown to form larger regions in Fig. 2d and e. The typical characteristics as described above, should come from the growth and migration of crystal nucleation originating from the carbon template. The precursor preferentially nucleates at the carbon sphere template. With low precursor concentration (i.e. Fe³⁺ 0.0375 and 0.075 mol/L), the concentration of template nucleation is limited. This leads to enhanced crystal growth, lowering the solute concentration, which further inhibits additional nucleation. Eventually the nucleation concentration is insufficient to form a complete structure. Instead, a damaged branching structure develops as shown in Fig. 2a and b. On the other hand, high precursor concentration (i.e. Fe³⁺ 0.1125 mol/L) results in a higher template nucleation concentration providing competition in the crystal growth phase. This leads to smaller GS, complete shell structures, and separate nanoparticles, as shown in Fig. 2c. When concentration of the precursor is raised even farther to ${\rm Fe}^{3+}$ 0.150 and 0.1875 mol/L, the heterogeneous nucleation sites provided by the carbon template are saturated, and homogeneous nucleation begins to occur. Evidence of this comes in the form of agglomerated nanoparticle regions shown by arrows e, f and g. In examining samples S4 and S5, it appears that the higher the precursor concentration, the larger the particle size and larger the agglomerated nanoparticle regions.

To investigate the influence of GS on the SR to ethanol gas, GS distributions were quantified, and the results are shown in Fig. 3. GS quantification was accomplished by selecting as many nanoparticles as possible in a TEM image, measuring their diameter and calculating the mean value. If the geometry of the nanoparticle is rodlike, the diameter is simply the shortest distance. If the geometry of the nanoparticle is subglobose, the mean value of several measurements spanning the nanoparticle at different locations is taken as the diameter. For S1, S2 and S3 (Fig. 3a-c, respectively), the GS are fit to a Gaussian distribution who's range becomes more narrow as the ratio of Fe3+ and carbon sphere templates come into better agreement resulting in less agglomerated nanoparticle regions. The standard deviation (Sta Dev) of GS for S1, S2 and S3 was found to be 4.8, 4.8, 4.2 nm respectively. This very narrow range of Sta Dev provides further evidence of a narrow GS distribution. For S4 and S5, a variation in GS is resultant from a combination of heterogeneous carbon sphere template nucleation and homogeneous nucleation. Homogeneous nucleation results in a very broad range of GS (Sta Dev for GS is 8.5 nm) as shown by the broad Gaussian distribution in Fig. 3e, while heterogeneous carbon sphere template nucleation results in a narrow Gaussian distribution (Sta Dev for GS is 4.0 nm) as shown in Fig. 3d. Fig. 3f indicates that sample S5 is a combination of heterogeneous and homogeneous nucleation as it has a wider distribution of GS than Fig. 3d. The average GS of S1, S2, S3, and S4 is 19.9 \pm 1.3, 17.3 \pm 1.7, 15.9 \pm 1.4 and 10.0 \pm 1.5 nm

Download English Version:

https://daneshyari.com/en/article/5448704

Download Persian Version:

https://daneshyari.com/article/5448704

Daneshyari.com